

Genetic deficiency and pharmacological modulation of ROR α regulate laser-induced choroidal neovascularization

Chi-Hsiu Liu¹, Felix Yemanyi¹, Kiran Bora¹, Neetu Kushwah¹, Alexandra K. Blomfield¹, Theodore M. Kamenecka², John Paul SanGiovanni³, Ye Sun¹, Laura A. Solt^{2,4}, Jing Chen¹

¹Department of Ophthalmology, Boston Children's Hospital, Harvard Medical School, Boston, MA 02115, USA

²Department of Molecular Medicine, UF Scripps Biomedical Research, Jupiter, FL 33458, USA

³BIO5 Institute and Department of Nutritional Sciences, University of Arizona, Tucson, AZ 85719, USA

⁴Department of Immunology and Microbiology, UF Scripps Biomedical Research, Jupiter, FL 33458, USA

Correspondence to: Jing Chen; email: jing.chen@childrens.harvard.edu

Keywords: age-related macular degeneration, angiogenesis, choroidal neovascularization, inflammation, nuclear receptors, ROR α , VEGFR2, TNF α

Received: July 20, 2022

Accepted: December 29, 2022

Published: January 10, 2023

Copyright: © 2023 Liu et al. This is an open access article distributed under the terms of the [Creative Commons Attribution License](https://creativecommons.org/licenses/by/3.0/) (CC BY 3.0), which permits unrestricted use, distribution, and reproduction in any medium, provided the original author and source are credited.

ABSTRACT

Choroidal neovascularization (CNV) causes acute vision loss in neovascular age-related macular degeneration (AMD). Genetic variations of the nuclear receptor RAR-related orphan receptor alpha (ROR α) have been linked with neovascular AMD, yet its specific role in pathological CNV development is not entirely clear. In this study, we showed that *Rora* was highly expressed in the mouse choroid compared with the retina, and genetic loss of ROR α in Staggerer mice (*Rora*^{sg/sg}) led to increased expression levels of *Vegfr2* and *Tnfa* in the choroid and retinal pigment epithelium (RPE) complex. In a mouse model of laser-induced CNV, ROR α expression was highly increased in the choroidal/RPE complex post-laser, and loss of ROR α in *Rora*^{sg/sg} eyes significantly worsened CNV with increased lesion size and vascular leakage, associated with increased levels of VEGFR2 and TNF α proteins. Pharmacological inhibition of ROR α also worsened CNV. In addition, both genetic deficiency and inhibition of ROR α substantially increased vascular growth in isolated mouse choroidal explants *ex vivo*. ROR α inhibition also promoted angiogenic function of human choroidal endothelial cell culture. Together, our results suggest that ROR α negatively regulates pathological CNV development in part by modulating angiogenic response of the choroidal endothelium and inflammatory environment in the choroid/RPE complex.

INTRODUCTION

Choroidal neovascularization (CNV) leads to rapid deterioration of visual function in neovascular age-related macular degeneration (AMD), a common and complex eye disease in the elderly. Abnormal growth of leaky choroidal vessels beneath the retina causes fluid exudation and edema, thereby resulting in retinal detachment and vision loss [1]. While CNV affects only about 10% of AMD patients, it causes up to 90% of vision loss associated with AMD. Both angiogenic and

inflammatory factors contribute to CNV, with vascular endothelial growth factor (VEGF) and its signaling being the most well studied [2–5]. Intraocular injections of anti-VEGF compounds have been successful in treating neovascular (wet) AMD, yet many patients remain unresponsive to these therapies, suggesting additional factors are at work. Development of invasive CNV requires not only elevated VEGF levels [2–5], but also an increased inflammatory state in the eye which is associated with invasion of inflammatory cells [6–8]. Many inflammatory mediators such as TNF α are also

linked with the development of CNV [8–10]. In addition, higher dietary fat intake [11, 12] and impaired lipid transport [13] are implicated in AMD. Both free and oxidized lipid metabolites including cholesterol and ApoB-containing lipoproteins are found in human drusen [14–16], a hallmark of AMD, suggesting a close link between lipid metabolism and AMD.

Retinoic acid receptor-related orphan receptor alpha (ROR α) is a lipid-sensing nuclear receptor that can bind cholesterol and other cholesterol-derived oxysterols [17, 18], although whether these are physiological ligands is still under investigation. Genetic variations in ROR α are linked with a higher risk of developing neovascular AMD in humans [19–21]. Functioning as a transcription factor, ROR α is a critical regulator of many biologic processes including circadian rhythm, eye and cerebellar development, regulation of lipid metabolism and inflammation [22, 23]. It mediates the expression of key enzymes and factors in lipid metabolism [24–26], and is also important for immunity and inflammatory disorders [22, 27–30]. Ligand binding regulates the interaction of ROR α with its transcriptional co-activators and/or co-repressors, the balance of which controls its resultant transcriptional activity [22]. Upon binding to a specific ROR response elements (RORE) in the regulatory region of target genes, ROR α and its cofactors together mediate the expression of target genes to impact cellular processes [22].

In the retina, ROR α has been localized in retinal neurons including retinal ganglion cells (RGC) and photoreceptors [31–33]. Our previous work found that ROR α is expressed in both inflammatory cells, including retinal macrophages and microglia, and RGCs and regulates pathological retinal angiogenesis in a mouse model of oxygen-induced retinopathy modeling ischemic proliferative retinopathy [34, 35]. Whether ROR α regulates CNV development remains unclear and is the focus of the current study.

Here, we investigated whether ROR α regulates CNV using a mouse model of laser-induced CNV, mimicking the neovascular features of wet AMD. We found that expression of ROR α was enriched in the mouse choroid/RPE complex and upregulated in laser-induced CNV. In *Staggerer* mice (*Rora*^{sg/sg}) with spontaneous mutation of ROR α resulting in loss of its function [36], genetic deficiency of ROR α significantly increased the size of laser-induced CNV lesions and associated vascular leakage. Treatment with an inverse agonist of ROR α also worsened laser-induced CNV. Both genetic loss and pharmacological inhibition of ROR α enhanced vascular expansion in choroidal explants *ex vivo*. Modulation of ROR α also directly impacted choroidal

vascular endothelium angiogenesis. Mechanistically, we found that loss of ROR α led to upregulation of VEGF receptor 2 (VEGFR2) and TNF α in mouse choroidal/RPE complex under normal conditions and following laser-induced CNV. These observations suggest that ROR α may negatively regulate pathological CNV through modulation of both angiogenic and inflammatory pathways.

MATERIALS AND METHODS

Animals

All animal studies were approved by the Institutional Animal Care and Use Committee at Boston Children's Hospital. The studies also adhered to the Association for Research in Vision and Ophthalmology Statement for the Use of Animals in Ophthalmic and Vision Research. Heterozygous mutant *Staggerer* (*Rora*^{+sg}), B6.C3(Cg)-*Rora*^{sg/J}, mice (stock no. 002651) were purchased from Jackson Laboratory (Bar Harbor, ME, USA) and bred to produce age-matched wild type (WT) and homozygous mice for this study. In addition, C57BL/6J mice (stock no. 000664, Jackson Lab) were used for agonist treatment experiments.

Laser-induced CNV

Laser photocoagulation was performed with Micron IV imaging system (Phoenix Research Lab, Pleasanton, CA, USA) as previously described [37, 38]. Briefly, young adult (2–3 months old) male *Rora*^{sg/sg} and WT mice were anesthetized. Male mice were used to avoid influence of sex-hormone on biological variations of CNV response in female mice as reported previously [37, 39]. After pupil dilation, each eye received four laser burns spaced evenly around the optic disc. The laser rupture of Bruch's membrane was confirmed by the presence of a vapor bubble. Lesions with no observation of bubbles and malformed lesions (fused, or with hemorrhage) were excluded from the study based on previously established criteria [37]. Seven (7) days post-laser, CNV was analyzed in choroidal flat mounts with isolectin B₄ (Invitrogen, I21413) staining to visualize and quantify lesion size. In addition, before euthanizing mice, fundus fluorescein angiography was performed and the severity of CNV lesion leakage was graded [40].

For pharmacological modulation of ROR α , injection of ROR α inverse agonist (SR3335) and agonist (SR1078) was performed in 6–8-week-old male C57BL/6J mice with daily i.p. injection (b.i.d.) from day 0–7 post-laser, at a dose of 15 mg/kg (body weight) for both compounds [41, 42]. Both compounds were synthesized and provided by coauthors T.M.K. and L.A.S.'s groups at the Scripps [43].

Fluorescein fundus angiography (FFA)

Fluorescein angiography was performed 7 days after the laser photocoagulation [37]. Photographs were taken with Micron IV imaging system after injection of Fluorescein AK-FLUOR (100 mg/ml, NDC 17478-101-12, Akorn, Lake Forest, IL, USA). AK-FLUOR stock was diluted to 10 mg/mL working solution and injected i.p. at 10 μ L/g (mouse body weight). The lesions were graded as described previously [40], on an ordinal scale defined by the spatial and temporal pattern of hyperfluorescence: grade 0 (no leakage); grade 1 (questionable leakage); grade 2A (leaky); grade 2B (pathologically significant leakage).

Choroidal sprouting assay

Sprouting of isolated choroidal explants was assayed as previously described [38, 44]. Peripheral parts of the choroid & sclera layer isolated from 6-8-week-old mice were cut into small pieces. Choroidal explants were then grown at 37°C with 5% CO₂ on growth factor-reduced Matrigel (30 μ L/well; BD Biosciences, San Jose, CA, USA) in 24-well plates containing CSC complete medium (Cell Systems, Kirkland, WA, USA) with media change every other day. Images of explants were taken 4 days after plating using a ZEISS AxioObserver.Z1 microscope. The area of explant sprouting was quantified with ImageJ using a semi-automated macro plug-in. Treatment with ROR α inverse agonist (SR3335) and agonist (SR1078) (5 μ M) or DMSO as control were performed in C57BL/6J choroidal explants.

Human choroidal endothelial cell (hCEC) culture and MTT and migration assays

HCECs were purchased (Celprogen, 36052-03) and cultured in endothelial cell complete medium (M36052-03S, Celprogen) on extra-cellular matrix coated dishes (Celprogen) according to vendor instruction. Cells between passage number 4 and 7 were treated with SR3335, SR1078 (both 10 μ M) or vehicle DMSO. Cell viability and/or proliferation was assessed after treatment using an MTT (3-(4,5-dimethylthiazol-2-yl)-2,5-diphenyltetrazolium bromide) cell metabolic activity assay kit (V13154, Fisher Scientific) as described previously [45]. Cell migration assay was carried out according to previous protocols [46].

Tissue and cell preparation for real time quantitative polymerase chain reaction (RT-qPCR)

Mouse choroidal sample preparation for RNA includes RPE/choroidal/sclera complex dissected from the eye ball. RPE RNA was isolated and purified from dissected

WT eye cups after removal of the retina following previous protocol [47]. Macrophage cells were murine RAW 264.7 cells (TIB-71, ATCC). Human microvascular endothelial cells (hRMEC) were purchased from Cell system (ACBRI 181) and mouse brain smooth muscle cells (mSMC) were from Cell Biologics (C57-6085). Cells were cultured according to vendor instructions respectively.

Total RNA was isolated from the homogenized mouse eye tissues or cells by PureLink™ RNA Mini Kit (Invitrogen) according to the manufacturer's instructions. Synthesis of cDNA was done by reverse transcription with iScript™ Reverse Transcriptase (Bio-Rad, Hercules, CA, USA). Quantitative analysis of gene expression was carried out by RT-qPCR using a C1000 Thermal Cycler (Bio-Rad) and the 2X SYBR Green qPCR Master Mix (bimake.com; Houston, TX, USA) with primers for specific genes. Copy number of each target gene cDNA was normalized to the house keeping genes, *Rn18s* or *Gapdh*, using comparative CT ($\Delta\Delta$ CT) method.

Mouse primers used are listed below:

Rora, forward: 5'-TCCCACCTGGAAACCTGCCAGT-3', reverse: 5'-ATGCGAGCTCCAGCCGAGGT-3';
Rn18s: forward: 5'-CACGGACAGGATTGACAGATT-3', reverse: 5'-GCCAGAGTCTCGTTTCGTTATC-3';
Gapdh: forward: 5'-AACAGCAACTCCCCTCTTC-3', reverse: 5'-CCTGTTGCTGTAGCCGTATT-3'.

Inflammatory genes: *Il-1b*, forward: 5'-TTCAGGCAG GCAGTATCACTC-3', reverse: 5'-GAAGGTCCACGG GAAAGACAC-3'; *Il-6*, forward: 5'-TAGTCCTTCCTA CCCCAATTTCC-3', reverse: 5'-TTGGTCCCTTAGCC ACTCCTTC-3'; *Nfkb1*, forward: 5'-GGAGAGTCTGA CTCTCCCTGAGAA-3', reverse: 5'-CGATGGGTTC GTCTTGGT-3'; *Nlrp3*, forward: 5'-ATTACCC GCCCGAGAAAGG-3', reverse: 5'-TCGCAGCAA GATCCACACAG-3'; *Tnfa*, forward: 5'-TCCAGTAG AATCCGCTCTCCT, reverse: 5'-GCCACAAGCA GGAATGAGAAG-3'.

Angiogenesis genes: *Ang1*, forward: 5'-AGCTCCACC TCGGGTCTACC-3', reverse: 5'-TGGTCACTCTGGA TCTCATTGG-3'; *Cxcr4*, forward: 5'-AGCCTGTGGA TGGTGGTGTTC-3', reverse: 5'-CCTTGCTTGATG ACTCCCAAAG-3'; *Dll4*, forward: 5'-TTCCAGGCA ACCTTCTCCGA-3', reverse: 5'-ACTGCCGCTATTC TTGTCCC-3'; *Flt1*, forward: 5'-GTCACAGATGTG CCGAATGG-3', reverse: 5'-TGAGCGTGATCAGCT CCAGG-3'; *Fzd4*, forward: 5'-TTCCTTTGTTCCGGT TTATGTGCC-3', reverse: 5'-CTCTCAGGACTGGT TCACAGC-3'; *Kdr (Vegfr2)*, forward: 5'-TTTGGA AATAACAACCCTTCAGA-3', reverse: 5'-GCTCCAGT

ATCATTTCACCA-3'; *Notch1*, forward: 5'-CCCTTGCTCTGCCTAACGC-3', reverse: 5'-GGAGTCCTG GCATCGTTGG-3'; *Pdgf*, forward: 5'-TGTGCCCATTCGCAGGAAG-3', reverse: 5'-GAGGTATCTCGTAAATGACCGTC-3'; *Plxnd1*, forward: 5'-GCTGACTGTA GCCTATGGGGA-3', reverse: 5'-GCCATCTGGTGGATGTCAT-3'; *Tspan12*, forward: 5'-TGCTTGGA TGAGGGACTACC-3', reverse: 5'-AACGTTCCGAAGTACCATGC-3'; *Vegfa*, forward: 5'-GGAGACTCTTCGAGGAGCACTT-3', reverse: 5'-GGCGATTTAGCAGCAGATATAAGAA-3'.

Human primers used are listed below:

RORA, forward: 5'-ACTCCTGTCTCGTCAGAAGA-3', reverse: 5'-CATCCCTACGGCAAGGCATTT-3'; *GAPDH*, forward: 5'-CCCTTCATTGACCTCAACTACA-3', reverse: 5'-ATGACAAGCTTCCCGTTCTC-3'.

Western blot analysis

Choroid/RPE complex was isolated from dissected mouse eyes at 1, 3, 5, and 7 days post-laser photocoagulation. Tissues were lysed in RIPA buffer (Thermo Scientific) with protease inhibitors and phosphatase inhibitors (Sigma-Aldrich). Total protein concentration was determined via a bicinchoninic acid (BCA; Thermo Fisher Scientific, 23227) assay. Equal amounts of protein lysates were then denatured using a 1:10 mixture of 2-mercaptoethanol and 4X Laemmli buffer, followed by heating to 100°C for 5 minutes. After SDS-PAGE separation, proteins were transferred to polyvinylidene fluoride (PVDF) membranes and probed with ROR α antibody (Abcam, ab60134), VEGFR2 antibody (R&D Systems, AF644), TNF α antibody (Cell Signaling Technology (CST), 11948), and β -actin antibody (CST, 3700). Secondary antibodies used are: HRP-conjugated mouse IgG, rabbit IgG (GE Healthcare UK Limited, NA9310V and NA934V, respectively) and goat IgG (SouthernBiotech, 6160-05). ECL Chemiluminescent Substrate Reagent Kit (Invitrogen) was used to generate signal for densitometry quantification.

Retinal cross section and immunohistochemistry

Mouse eyes were enucleated and fixed in 4% paraformaldehyde in PBS at room temperature for 1 hour, followed by embedding in optimal cutting temperature (OCT) compound, and frozen for cryosection. Immunohistochemistry on retinal sections was performed as described in previous protocols [35, 48]. Primary antibodies for ROR α (Abcam, ab278099) were used and sections were costained with isolectin B₄ (Invitrogen, I21413) overnight at 4°C. After washing, the retinas were incubated with secondary antibody

(Thermo Fisher, A11034) for 1 hour at room temperature followed by imaging with a fluorescence microscopy (Axio Observer Z1, Carl Zeiss Microscopy).

Statistical analysis

Quantitative data are presented as means \pm SEM (standard error of the mean), with the exception of qPCR results, which are represented as the mean \pm SD (standard deviation). Asterisks represent the *P*-value according to two-tailed Student's *t*-test (2 groups), One-way ANOVA (more than 2 groups), or Two-way ANOVA (two factors, more than 2 groups): **P* \leq 0.05; ***P* \leq 0.01; ****P* \leq 0.001; *****P* \leq 0.0001.

Data and materials availability

The paper contains all methods and data needed to evaluate the conclusions. Additional related data and materials are available upon request.

RESULTS

ROR α was enriched in the mouse choroid and regulated expression of angiogenic and inflammatory genes

We first compared relative gene expression levels of *Rora* in different mouse ocular tissues and cells. Expression of *Rora* mRNA was highly enriched in the normal choroid/RPE complex with about 6-fold increase compared with the retina (Figure 1A). Because the choroid/RPE complex also contains RPE and microglia/macrophages, we also compared *Rora* expression levels in isolated mouse RPE cells and cultured mouse macrophage (RAW264.7) cells, both of which showed lower expression levels than the combined choroid/RPE complex, suggesting that *Rora* is enriched in the mouse choroid (Figure 1A). Immunohistochemistry staining of eye cross sections also showed colocalization of ROR α antibody staining with isolectin-positive choroidal vessels, in addition to ROR α antibody staining in RPE (Figure 1B).

Next, we evaluated expression of inflammatory and angiogenic genes in ROR α -deficient (*Rora*^{sg/sg}) choroid/RPE complex. Expression of *Rora* mRNA was very low and barely detectable in *Rora*^{sg/sg} choroid/RPE compared with age-matched wild type (WT) controls (Figure 1C), confirming its genetic deficiency. Importantly, *Rora*^{sg/sg} choroid/RPE complex had much higher expression levels of inflammatory cytokines, with ~8-fold upregulation of *Tnfa* mRNA, in addition to upregulation of *Il1b*, *Il6*, *Il17a*, and *Nlrp3*, compared

with WT (Figure 1C). In addition, expression of VEGF receptor 2 (*Vegfr2*, or *Kdr*) was significantly higher with ~7-fold upregulation in *Rora*^{sg/sg} choroid/RPE complex (Figure 1D), while many other angiogenic-related factors (*Vegfa*, *Pdgf*, *Ang1*, and *Dll4*) and receptors (*Vegfr1*, *Plxnd1*, *Fzd4*, *Tspan12*, *Notch1&4*, and *Cxcr4*) were either unchanged or modestly down-regulated. These results indicate that ROR α may regulate expression of both angiogenic and inflammatory genes and loss of ROR α may promote an inflammatory and angiogenic environment around the choroid.

Genetic deficiency of ROR α worsened laser-induced CNV

To determine the role of ROR α in the regulation of CNV, we used a mouse model of laser-induced CNV to mimic the neovascular aspect of AMD (Figure 2A). Young adult (2–3-month-old) *Rora*^{sg/sg} and WT mice were exposed to laser-induced CNV model. At one

week post laser, *Rora*^{sg/sg} choroidal flat mounts showed greater than 2-fold increase in CNV lesion area compared to WT (Figure 2B, 2C). In addition, genetic deficiency of ROR α resulted in a higher percentage of leaky CNV lesions (Figure 2D, 2E). Over 78% of *Rora*^{sg/sg} CNV lesions were graded as leaky (including 37.5% of grade 1, 31.25% of grade 2A, and 9.38% of grade 2B lesions), while in WT mice the percentage of leaky lesions was approximately 58% (Figure 2D, 2E). These findings of larger, leakier, and hence more severe CNV lesions in ROR α -deficient mice suggest a negative regulatory role of ROR α in CNV formation.

Loss of ROR α upregulated VEGFR2 and TNF α protein levels in laser-induced CNV

Having established that loss of ROR α exacerbates laser-induced CNV, we next evaluated whether dysregulation of angiogenic and inflammatory genes such as VEGFR2 and TNF α as seen in normal *Rora*^{sg/sg} choroid may

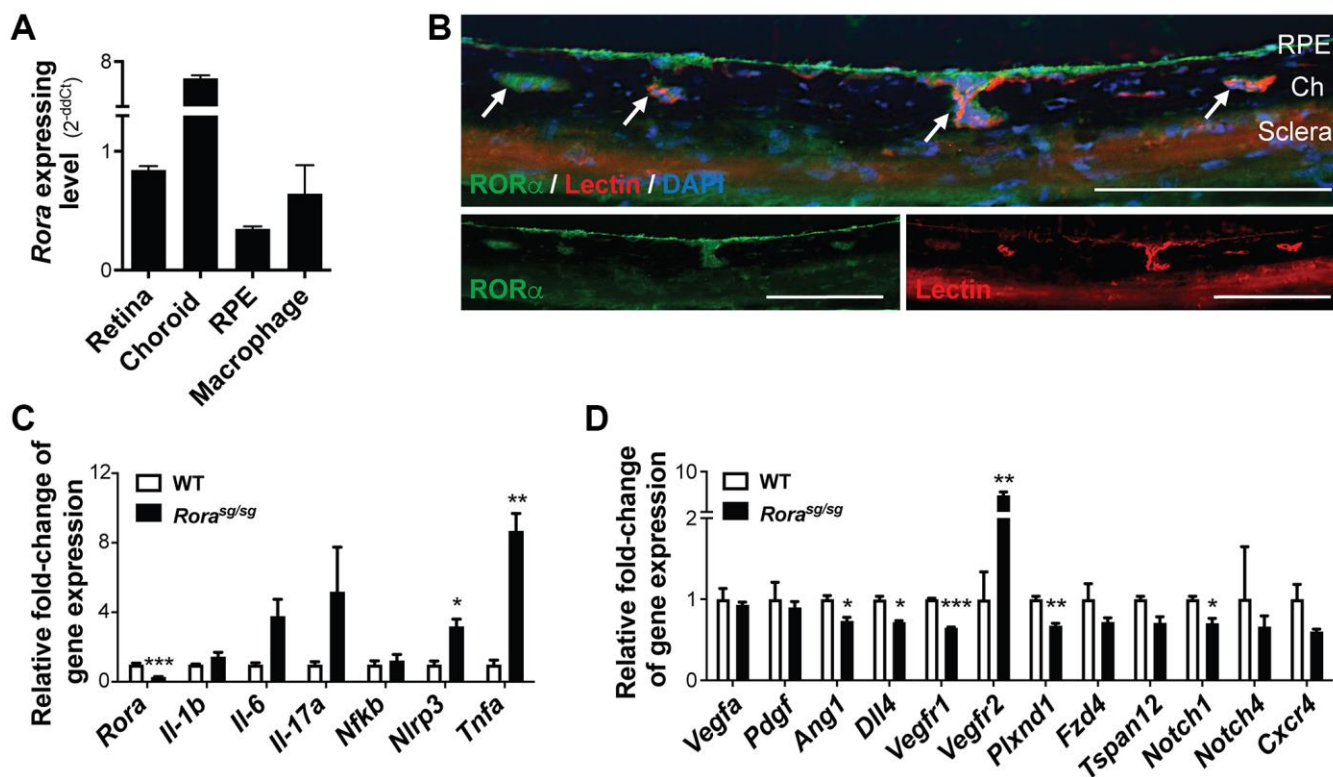


Figure 1. ROR α was enriched in mouse choroid and regulated inflammatory and angiogenic genes. (A) Relative *Rora* expression in different types of mouse ocular tissues, namely retina and RPE/choroid complex, and cells (isolated pure RPE from mouse eyes and RAW264.7 macrophage cell line) measured with quantitative RT-PCR and normalized to housekeeping gene *Rn18s*. The choroid complexes expressed the highest expression levels of *Rora* compared to the retinas, RPE, and macrophage cells ($n = 3$ /group). (B) Immunohistochemistry staining of retinal cross sections shows ROR α antibody staining (green), vascular endothelium marker isolectin (red), and DAPI (blue). Ch: choroid. Scale bars, 100 μ m. (C, D) q-PCR analysis for the expression of *Rora* and inflammatory (C) and angiogenic (D) genes in the RPE/choroid complexes from *Rora*^{sg/sg} and WT mice in normal condition without CNV showed that deficiency of ROR α led to significant increase in *Vegfr2* and *Tnfa* mRNA levels, in addition to changes in other inflammatory and angiogenic genes ($n = 3$ mice/group). Data are presented as means \pm SEM. * $P \leq 0.05$; ** $P \leq 0.01$; *** $P \leq 0.001$.

stimulate CNV formation. Protein levels of ROR α were highly upregulated over time at 1, 3, and 5 days after laser in C57BL/6J mice (Figure 3A, 3B), which may reflect hypoxia-stimulated ROR α expression in CNV after laser-induced tissue injury, since ROR α is known to be hypoxia-responsive.

Next we evaluated whether VEGFR2 and TNF α , both upregulated in *Rora*^{sg/sg} choroid/RPE complex (Figure 1C, 1D) are also affected in *Rora*^{sg/sg} eyes with CNV. VEGFR2 is a major receptor for VEGF, the main inducer of both clinical and experimental CNV [5]. On

the other hand, TNF α , a major inflammatory cytokine secreted by macrophages, T cells, vascular endothelium and neurons, also primes vascular endothelium for their angiogenic response [49]. We found that protein levels of VEGFR2 and TNF α were strongly upregulated in *Rora*^{sg/sg} vs. WT choroid/RPE complex 7 days after laser-induced CNV (Figure 3C, 3D), consistent with worsened CNV lesions in *Rora*^{sg/sg} eyes (Figure 2). Together, these findings suggest that genetic loss of ROR α may increase laser-induced CNV severity as the result of enhanced VEGFR2 and TNF α levels in the choroid/RPE complex (Figure 3D).

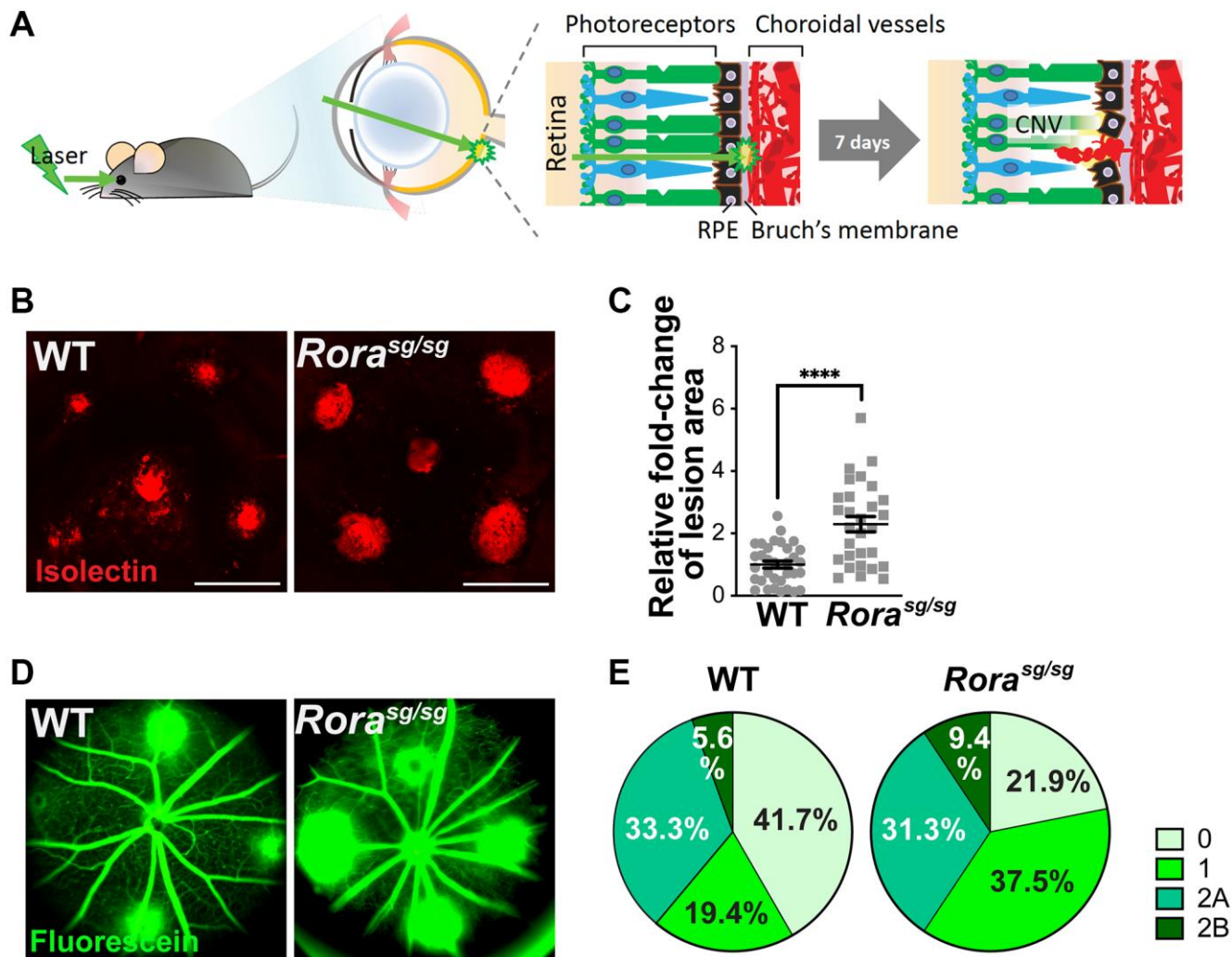


Figure 2. Genetic deficiency of ROR α increased lesion size and vascular leakage in a mouse model of laser-induced choroidal neovascularization (CNV). (A) A cartoon illustrating laser-induced CNV model in mice. Young adult mice are exposed to laser, which ruptures Bruch's membrane and causes CNV. (B) Representative images of choroidal flat mounts with laser-induced CNV from wild type (WT) and ROR α -deficient (*Rora*^{sg/sg}) mice stained with isolectin IB₄ (red) showing four lesions, with optic disc in the center. Scale bars, 500 μ m. (C) Quantification of the relative fold-change of CNV lesion areas showed that ROR α -deficient mice have larger CNV lesion sizes compared to age-matched WT ($n = 22$ – 23 eyes/group). Each data point represents averaged lesion size from one eye. Solid horizontal bars indicate means \pm SEM; **** $P \leq 0.0001$. (D) Representative images of fundus fluorescein angiography (FFA) from WT and *Rora*^{sg/sg} mice with laser-induced CNV at day 6 after laser photocoagulation. (E) Lesions were graded on an ordinal scale of the fluorescein (D; green) leakage appearance: grade 0 (no leakage); grade 1 (questionable leakage); grade 2A (leaky); grade 2B (pathologically significant leakage). *Rora*^{sg/sg} mice revealed much fewer grade 0 lesions and more grade 1, 2A and 2B lesions compared to WT mice ($n = 10$ mice/group).

Genetic loss and pharmacological inhibition of ROR α increased choroidal explant sprouting abilities *ex vivo*

To explore the effects of ROR α on choroidal angiogenic ability, we next performed *ex vivo* sprouting assays using mouse choroidal explants, which partly maintain the cellular matrix and environment in living choroid (Figure 4A). In line with the results from the *in vivo* laser-induced CNV model, choroidal explants isolated from *Rora*^{sg/sg} mice exhibited about 2-fold increase in sprouting abilities compared with the choroidal explants from age-matched WT (Figure 4B, 4C), suggesting increased choroidal angiogenic potential in the absence of ROR α .

To modulate ROR α pharmacologically, synthetic ROR α inverse agonist SR3335 [41] and ROR α/γ agonist SR1078 [42] were developed. These compounds can bind to the ligand binding domain of ROR α to modulate its transcriptional activity [43]. Choroidal explants treated with ROR α modulators showed results consistent with *Rora*^{sg/sg} mice, where choroidal explants treated with SR3335 to inhibit ROR α revealed significantly larger (~60%) sprouting areas compared with the vehicle controls, and ROR α activation with SR1078 treatment showed a trend of reduced sprouting ability *ex vivo* (Figure 4D, 4E). Together, these data

suggest that both genetic and pharmacological modulation of ROR α directly altered the angiogenic and sprouting ability of choroid.

Pharmacological modulation of ROR α affected laser-induced CNV lesions

To further corroborate the effects of ROR α on CNV, we administered pharmacological modulators of ROR α (inverse agonist SR3335 or agonist SR1078) to C57BL/6J mice (daily intraperitoneal injection) after laser-induced CNV (Figure 5A). SR3335 treatment for ROR α inhibition resulted in substantially increased CNV lesion size (Figure 5B, 5C), consistent with our findings in mice with systemic deficiency of ROR α (Figure 2). The administration of SR1078 for ROR α activation showed a trend of attenuated severity of CNV lesion size (Figure 5B, 5C). In addition, more CNV lesions with SR3335 treatment and less with SR1078 were graded as leaky in grade 1 and 2 (Figure 5D). One might note that the percentage of overall leaky lesion differs in control-treated C57BL/6J mice vs. WT mice (in Figure 2), potentially reflecting difference in mouse colony, FFA procedures and the inherent variability in the CNV model itself. Together these data indicating that pharmacological modulation of ROR α activities may influence the development of CNV and could serve as a potential strategy for controlling pathological CNV.

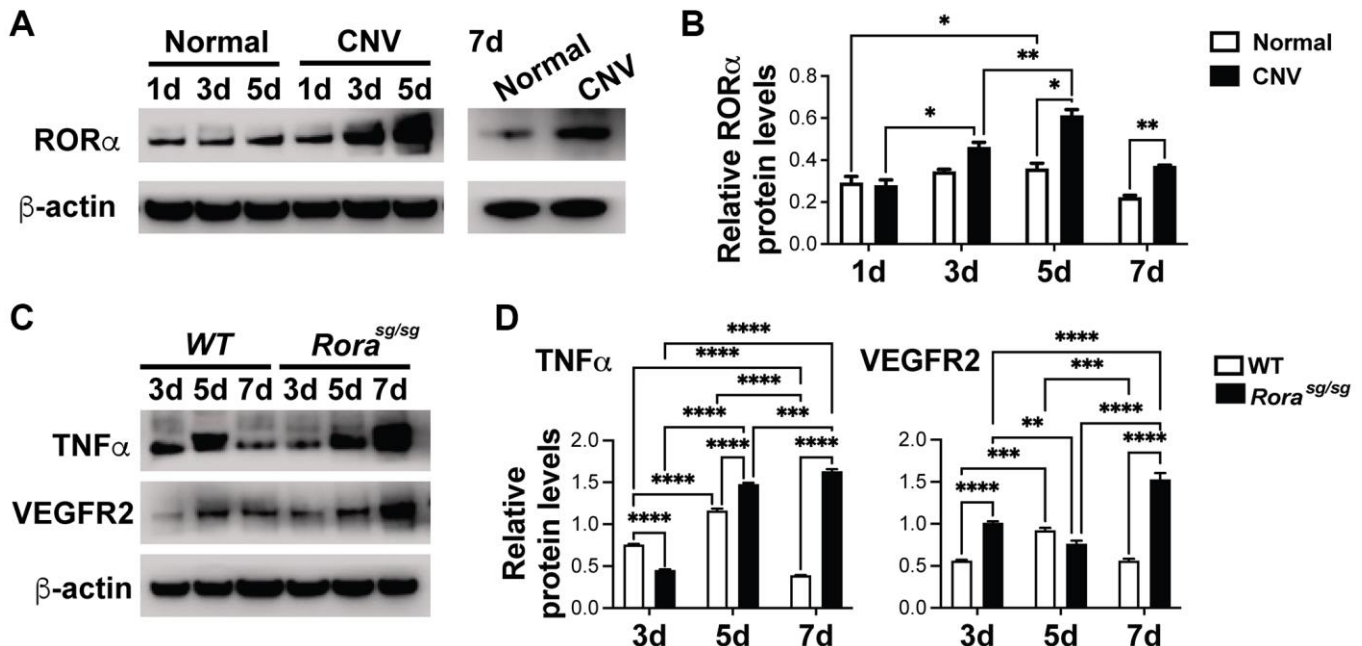


Figure 3. ROR α was induced in CNV and regulated VEGFR2 and TNF α levels in laser-induced CNV. (A, B) Western blotting images (A) and densitometric analysis (B) of protein levels of ROR α from choroid/RPE complexes with laser-induced CNV from C57BL/6J mice at 1, 3, 5 and 7 days (d) post-laser, compared with β -actin. β -actin served as loading control. Each band represents pooled sample from 3 retinas. $n = 3$ mice/group. (C, D) Western blotting images (C) and densitometric analysis (D) showing TNF α and VEGFR2 protein levels in choroid/RPE complexes at 3, 5, and 7 days after laser-induced CNV in *Rora*^{sg/sg} and WT eyes, compared with β -actin as loading control. Each band represents pooled sample from 3 retinas. $n = 3$ mice/group. * $P \leq 0.05$; ** $P \leq 0.01$; *** $P \leq 0.001$; **** $P \leq 0.0001$.

Angiogenic function of human choroidal endothelial cells was directly regulated by pharmacological modulation of ROR α

To evaluate whether ROR α may function directly in human choroidal endothelium, we first assessed relative mRNA expression levels of ROR α in human choroidal endothelial cells (hCECs), human microvascular endothelial cells (hRMECs), mouse brain smooth muscle cells (mSMCs) and whole mouse retina. Smooth muscle cells were examined because of their presence in choroid vascular tissue. ROR α mRNA was highly expressed in hCECs as compared with hRMECs, and expression of ROR α mRNA in mSMCs was barely

detectable (Figure 6A), confirming enrichment of ROR α in choroidal vascular endothelium.

Next, hCECs were treated with ROR α inverse agonist SR3335 or agonist SR1078. Choroidal endothelial cell viability and/or proliferation was assessed using MTT assay. We found that SR3335 treatment showed significant increase ($p \leq 0.05$) in cellular metabolic activity of hCECs as compared to the vehicle control, whereas a decreased trend was observed upon SR1078 treatment (Figure 6B). In addition, ROR α inhibition with SR3335 significantly promoted hCEC migration, and in contrast, ROR α activation with SR1078 suppressed hCEC migration (Figure 6C, 6D). These

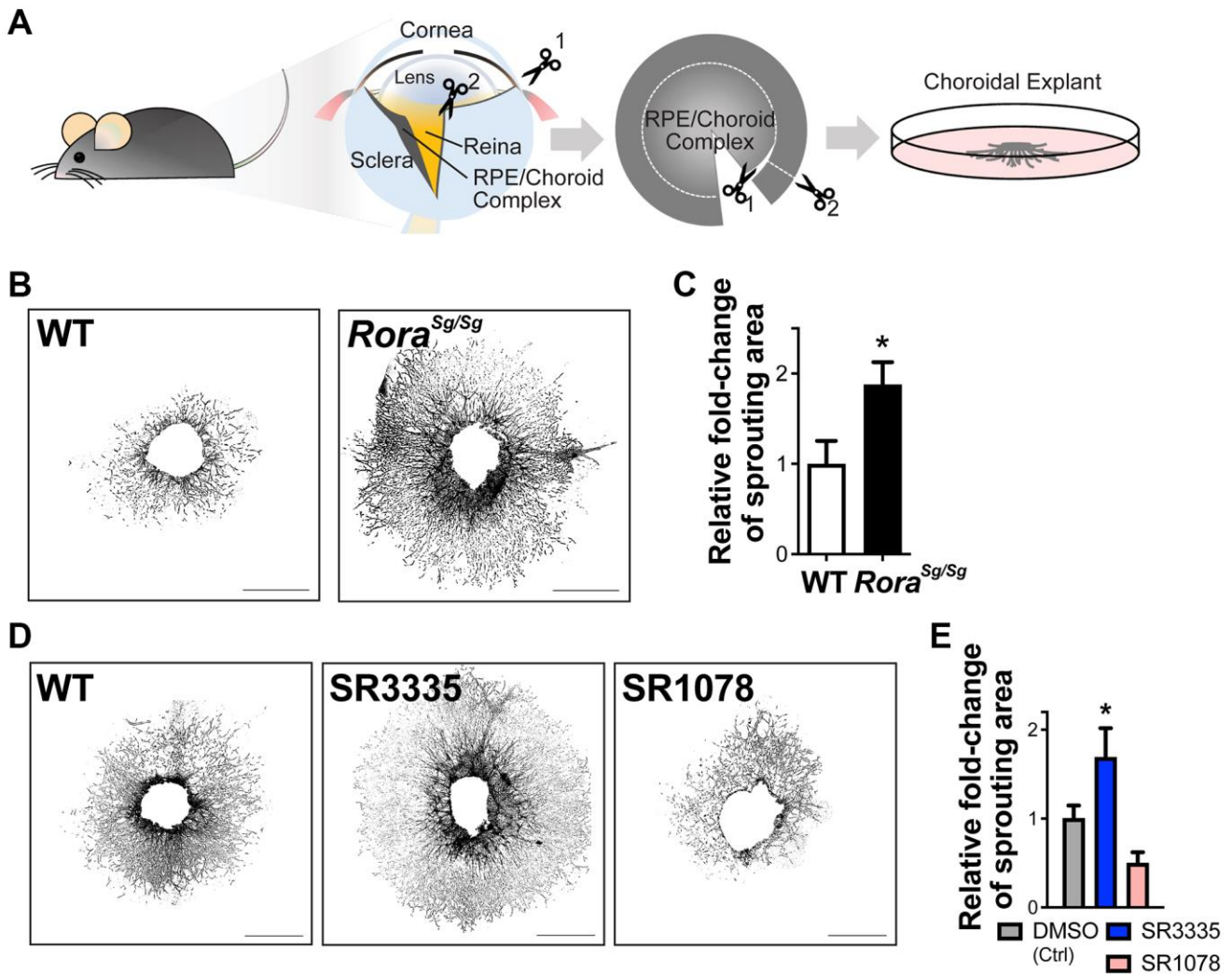


Figure 4. ROR α regulates choroidal sprouting *ex vivo*. (A) A cartoon illustrates the experimental steps of choroidal explant assay by isolation, dissection and culture of choroid fragments. (B) Representative images of choroidal sprouting assays from age-matched WT and *Rora^{Sg/Sg}* mice. Scale bars, 1 mm. (C) Quantitative analysis of the choroidal sprouting area from 5 days after explantation showed that *Rora^{Sg/Sg}* choroids have significantly increased sprouting ability *ex vivo* compared to WT. $n = 3-5$ mice (10-12 explants)/group. (D) Representative images of choroidal explants isolated from C57BL/6J mice and treated with SR3335 (ROR α inverse agonist), SR1078 (ROR α / γ agonist) or vehicle control DMSO (all at 5 μ M). Scale bars, 1 mm. (E) Quantification of the sprouting area indicated that inhibition of ROR α with SR3335 significantly increased choroidal sprouting area while SR1078 reduced the choroidal sprouting ability compared to the DMSO (control) treated group. $n = 3$ mice/group; 10-12 explants per treatment. Data are presented as mean \pm SEM. * $P \leq 0.05$.

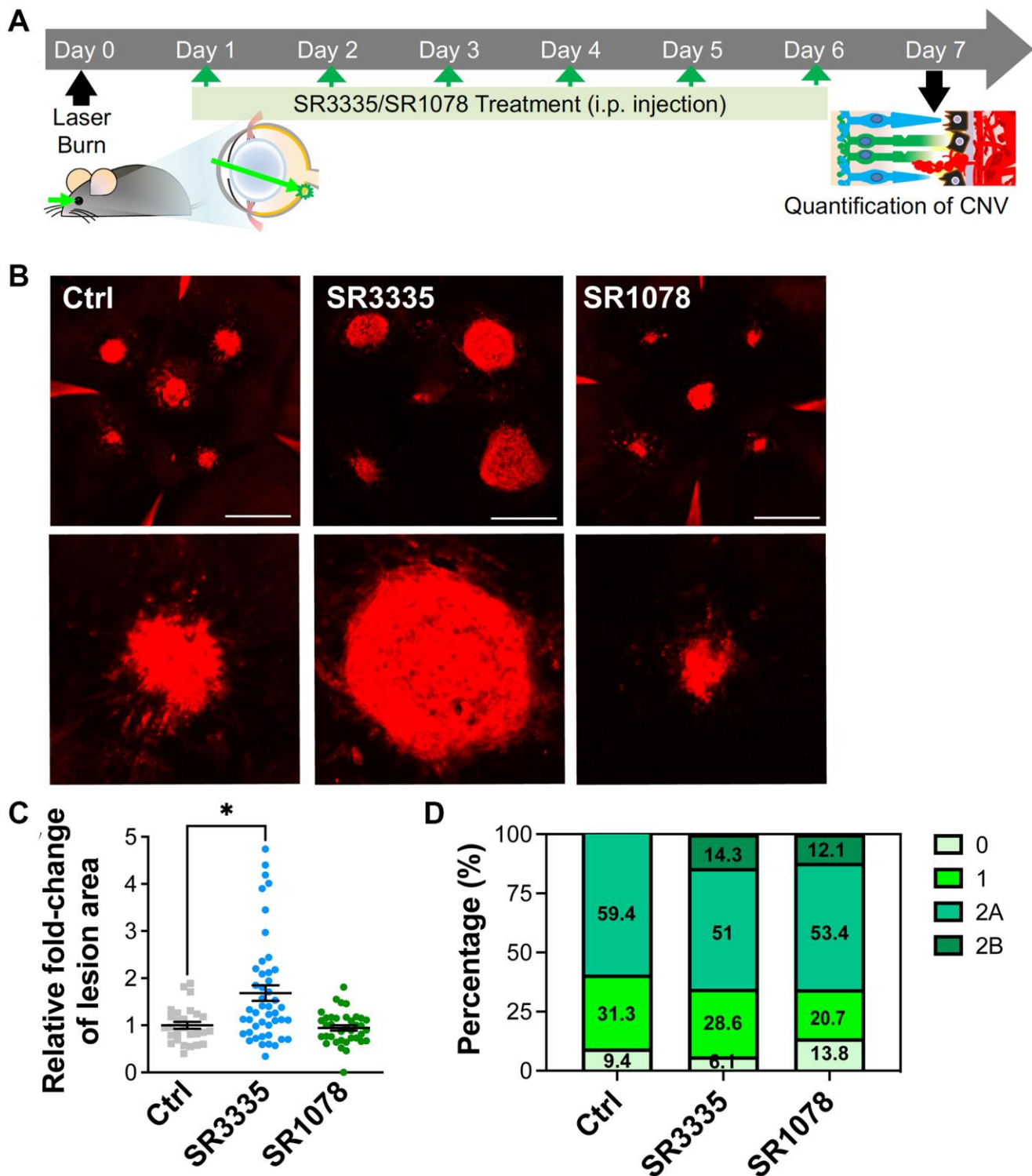


Figure 5. Pharmacological modulation of ROR α affects CNV lesion size in mice. (A) A cartoon of the drug treatment timeline in laser-induced CNV. ROR α inverse agonist (SR3335), agonist (SR1078), or vehicle control was intraperitoneally injected (daily) into C57BL/6J mice after laser-induced CNV. (B) Representative images of isolectin-stained (red) choroidal flat mounts, isolated from mice of all treatment groups on day 7 after laser photocoagulation. Scale bars, 500 μ m. (C) Quantification of isolectin-stained CNV area showed significantly increased CNV lesion size in the mice treated with SR3335, and while as the CNV lesion size in the SR1078-treated group did not show significant change, compared to the vehicle control treated group ($n = 5-8$ mice/group). (D) Vascular leakage from CNV lesions were assessed by fundus fluorescein angiography (FFA) at day 6 after laser photocoagulation and graded on an ordinal scale of the fluorescein leakage appearance: grade 0 (no leakage); grade 1 (questionable leakage); grade 2A (leaky); grade 2B (pathologically significant leakage). $n = 5-8$ mice/group. Data are presented as mean \pm SEM. * $P \leq 0.05$.

data suggest that pharmacological modulation of ROR α activities directly regulates choroidal angiogenesis in the vascular endothelium, which underlies the influence of ROR α on the development of CNV lesions.

DISCUSSION

In this study, we present findings for a protective role of ROR α in a mouse laser-induced CNV model of neovascular AMD. We found that the expression of ROR α was enriched in the mouse choroid and particularly choroidal endothelium, consistent with previous work finding presence of ROR α in human

aortic vascular endothelium [50]. Both genetic deficiency and pharmacological inhibition of ROR α worsened laser-induced CNV, suggesting an anti-angiogenic role of ROR α in CNV, in line with a previous study in a hind limb ischemia model that reported increased ischemia-induced angiogenesis in *Rora*^{sg/sg} mice [51]. Previously in an oxygen-induced retinopathy model and in *Vldlr*^{-/-} mice with spontaneous subretinal neovascularization, we found that either genetic loss or pharmacological inhibition of ROR α suppressed retinal neovascularization in neonatal mice [34]. These results together reflect distinct tissue-specific anti-angiogenic roles of ROR α in regulating

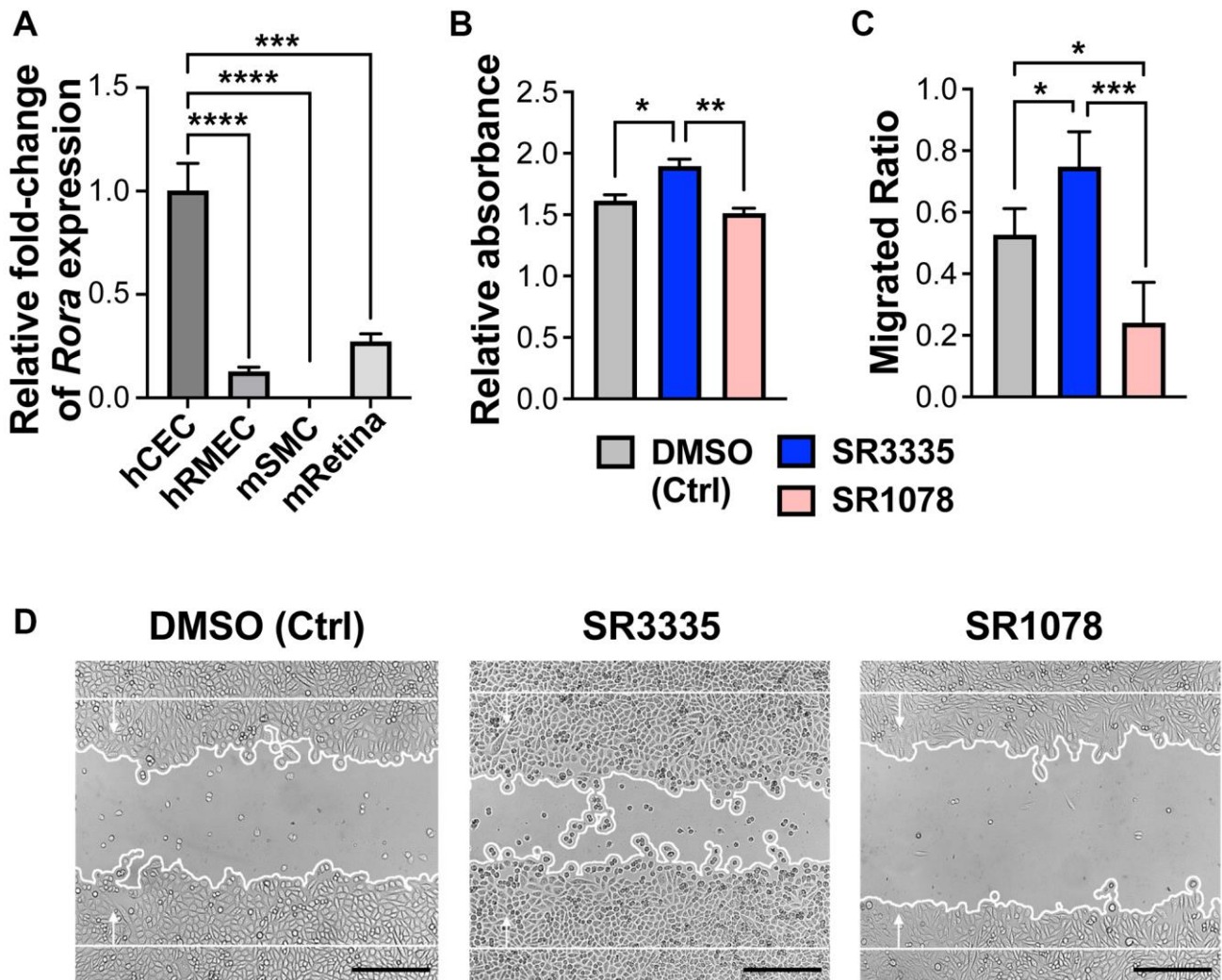


Figure 6. Pharmacological modulation of ROR α regulates human choroidal endothelial cell angiogenic function. (A) Relative mRNA expression of ROR α in human choroidal endothelial cell (hCEC), human retinal microvascular endothelial cell (hrMEC), mouse brain smooth muscle cell (mSMC) and mouse whole retina (mRetina), measured with quantitative RT-PCR and normalized to housekeeping gene *GAPDH* (human) and *Gapdh* (mouse) respectively. $n = 3/\text{group}$. (B) HCECs were treated with ROR α inverse agonist (SR3335), agonist (SR1078), or DMSO vehicle control. MTT assay was performed to evaluate cell viability and proliferation. Cell growth was calculated as fold change of relative absorbance normalized to the values at 0 hr. $n = 3/\text{group}$. (C, D) Quantification analysis (C) and representative images (D) of hCEC migration assay. Cells were grown to confluence and treated with SR3335, SR1078, or DMSO vehicle control. Mitomycin was used to inhibit cell proliferation. A scratch wound was generated in the cells. Cell migration were measured after 24 hr and quantified as new cell coverage areas normalized by the original wound areas. $n = 4/\text{group}$. Scale bar: 250 μm . * $P \leq 0.05$; ** $P \leq 0.01$; *** $P \leq 0.001$; **** $P \leq 0.0001$.

adult tissue angiogenesis in the choroid and peripheral organs, which may differ from its pro-angiogenic role in neonatal retinal vasculature under pathological conditions. Indeed, $ROR\alpha$ is expressed in much higher levels in choroidal endothelium than in retinal microvascular endothelium (Figure 6). In addition, $ROR\alpha$ deficiency stimulated a pro-inflammatory environment in the CNV choroid in this study, whereas in the oxygen-induced retinopathy model [34], $ROR\alpha$ deficiency lead to an anti-inflammatory profile in neonatal retinas. These endothelial specific and inflammatory difference together may underlie in part the different vascular response to $ROR\alpha$ in the two ocular vascular beds and angiogenesis models.

$Rora^{sg/sg}$ choroid with CNV exhibited enhanced levels of VEGFR2 and $TNF\alpha$ proteins, which may explain the exacerbated laser-induced CNV lesions. VEGFA is the major inducer of CNV in wet AMD and also the most important angiogenic factor in experimental CNV [5]. While loss of $ROR\alpha$ did not significantly alter expression of *Vegfa*, it enhanced VEGFR2 expression

and thereby VEGF signaling response, which contributes to CNV formation. Other angiogenesis-related genes including VEGFR1 showed modest changes in mRNA levels suggesting their potentially limited impact. VEGFR2 is expressed abundantly in vascular endothelium including the choroid, and $ROR\alpha$ expression was also found to be enriched in the choroid, suggesting a vascular specific role $ROR\alpha$ of choroidal $ROR\alpha$ in regulating CNV. This notion is consistent with our findings in *ex vivo* choroidal explants and hCECs, where genetic loss and pharmacological inhibition of $ROR\alpha$ both promoted vascular growth in choroidal explants, and $ROR\alpha$ modulation directly regulated hCEC angiogenesis. In addition, $TNF\alpha$ protein levels were also upregulated in $Rora^{sg/sg}$ choroid, along with several other inflammatory cytokines and factors such as *Nlrp3*, further promoting the choroidal inflammatory environment to potentially sensitize VEGF response and exacerbate CNV (Figure 7). Previously, inhibition of VEGF or $TNF\alpha$ was found to block or reduce laser-induced CNV in a monkey model [52]. Together our findings suggest that $ROR\alpha$ may regulate both VEGF

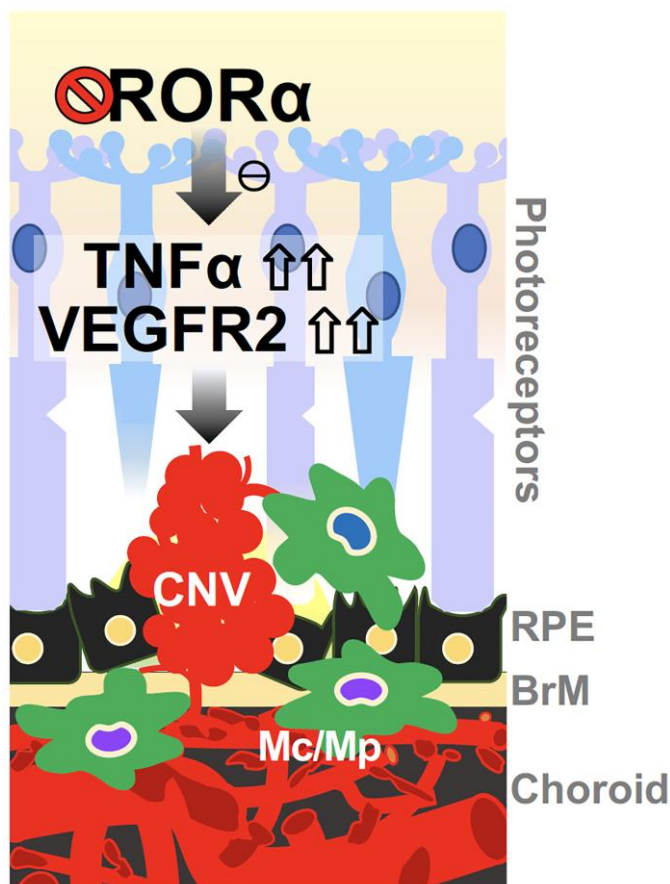


Figure 7. A schematic model for the effects of $ROR\alpha$ on regulating CNV in wet AMD. Deficiency of $ROR\alpha$ in choroid vessels directly induces expression of VEGF receptor VEGFR2, leading to enhanced choroidal endothelial angiogenic response and exacerbated pathological CNV formation. $ROR\alpha$ deficiency may also influence CNV via increased $TNF\alpha$, and chronic inflammation in the choroidal local environment, to potentially sensitize VEGF angiogenic response and thereby CNV formation. Abbreviations: BrM: Bruch's membrane; CNV: choroidal neovascularization; Mc: microglial cell; Mp: macrophage; RPE: retinal pigment epithelium.

and TNF α to regulate both angiogenesis and inflammation in CNV. Previously in an oxygen-induced retinopathy model we found that genetic deficiency of ROR α regulates macrophage polarization and retinal inflammation with dampened TNF α [34]. ROR α also plays a critical role in regulating T_H17-driven inflammatory disorders [27, 30], suggesting a diverse and tissue-dependent role of ROR α in inflammation regulation. As a constitutively active transcription factor, it is unclear through what mechanisms loss of ROR α induced upregulation of VEGFR2, TNF α and other downstream factors. Whether this reflects direct transcriptional repression through potentially negative response elements [53] on their RORE sites, or indirect regulation via other intermediate factors will await further studies.

We found enriched levels of ROR α in the mouse choroid and human choroidal vascular endothelial cell culture, consistent with a recent report of nuclear receptor atlas showing abundant levels of ROR α in freshly isolated choroid and primary choroidal endothelial cells from human donors [54]. ROR α was also present in RPE and macrophages. Macrophages contribute greatly to formation of CNV [55], whereas RPE, a main producer of secreted VEGF, also influences CNV formation significantly. Therefore, potential cell-specific contribution of ROR α from RPE or inflammatory cell sources towards the observed CNV effects cannot be excluded. In addition, localization of ROR α was also reported in retinal neurons such as RGCs [33, 35] and cone photoreceptors [56], although the relative contribution of ROR α in these retinal neurons in CNV formation is likely limited. Choroid tissue also contains smooth muscle cells, although our analysis of mouse brain smooth muscle cells showed undetectable levels of ROR α expression (Figure 6). A previous study found ROR α expression in human aortic smooth muscle cells [50], hence ROR α expression in smooth muscle cells may be organ- or species-dependent. Additional investigation exploring the cell specific contribution of ROR α in CNV will help address this limitation of the current study. Studying other potential molecular targets of ROR α in CNV is also needed in future work, as well as the physiological roles of natural ROR α ligands in CNV formation.

The natural ligands for ROR α are cholesterol derivatives, and ROR α regulates cholesterol homeostasis in the liver [57]. Dyslipidemia is closely linked with clinical AMD, and both cholesterol and cholesteryl fatty acid esters are found to be highly concentrated in the extracellular milieu around Bruch's membrane and enriched in drusen [58]. One of them, 7-ketocholesterol, accumulates with age in ocular tissues and in drusen

[58] and promotes choroidal endothelial cell migration and neovascularization by inducing endothelial-mesenchymal transition [58]. ROR α may be the link between these cholesterol metabolites and choroidal angiogenesis and inflammation, leading to worsened CNV in the absence of ROR α .

Pharmacological modulation of ROR α with a synthetic agonist and inverse agonist regulated vascular growth in choroidal explants and in laser-induced CNV, suggesting ROR α may be a potential druggable target for managing CNV. ROR α may target both angiogenic and inflammatory pathways, which can offer more advantage than targeting a single pathway. While SR1078 only showed limited protection towards choroidal explant and CNV in this work, future development of more potent or more efficient ROR α -specific agonists may provide better protection. Currently, AAV-delivery of ROR α (OCU410) is being evaluated by Ocugen Inc. (Malvern, PA, USA) as a potential dry AMD treatment with a planned clinical trial. Targeting ROR α and its related pathway may thus provide a new way to tackle CNV in late neovascular AMD or even early dry AMD by addressing both angiogenic and inflammatory pathogenic factors, which can offer more advantage than targeting a single pathway.

AUTHOR CONTRIBUTIONS

C.-H.L. and J.C. conceived and designed the study; C.-H.L. and J.C. wrote the manuscript. C.-H.L., F.Y., K.B., N.K., A.K.B., and Y.S. performed experiments and collected and analyzed the data; T.M.K., L.A.S., J.P.S. and Y.S. shared reagents and resources and provided expert advice; all authors edited and approved the manuscript.

ACKNOWLEDGMENTS

We thank Drs. Lois E.H. Smith, Zhongjie Fu, Yohei Tomita and Tianxi Wang for helpful discussion and technical assistance.

CONFLICTS OF INTEREST

The authors declare no conflicts of interest related to this study.

ETHICAL STATEMENT

All animal studies were approved by the Institutional Animal Care and Use Committee at Boston Children's Hospital. The studies also adhered to the Association for Research in Vision and Ophthalmology Statement for the Use of Animals in Ophthalmic and Vision Research.

FUNDING

This work was supported by NIH/NEI R01 grants (EY024963, EY028100, and EY031765), BrightFocus Foundation, Boston Children's Hospital Ophthalmology Foundation, and Mass Lions Eye Research Fund Inc. (to J.C.).

REFERENCES

1. Lim LS, Mitchell P, Seddon JM, Holz FG, Wong TY. Age-related macular degeneration. *Lancet*. 2012; 379:1728–38.
[https://doi.org/10.1016/S0140-6736\(12\)60282-7](https://doi.org/10.1016/S0140-6736(12)60282-7)
PMID:[22559899](https://pubmed.ncbi.nlm.nih.gov/22559899/)
2. Ishibashi T, Hata Y, Yoshikawa H, Nakagawa K, Sueishi K, Inomata H. Expression of vascular endothelial growth factor in experimental choroidal neovascularization. *Graefes Arch Clin Exp Ophthalmol*. 1997; 235:159–67.
<https://doi.org/10.1007/BF00941723>
PMID:[9085111](https://pubmed.ncbi.nlm.nih.gov/9085111/)
3. Honda M, Sakamoto T, Ishibashi T, Inomata H, Ueno H. Experimental subretinal neovascularization is inhibited by adenovirus-mediated soluble VEGF/flt-1 receptor gene transfection: a role of VEGF and possible treatment for SRN in age-related macular degeneration. *Gene Ther*. 2000; 7:978–85.
<https://doi.org/10.1038/sj.gt.3301203>
PMID:[10849558](https://pubmed.ncbi.nlm.nih.gov/10849558/)
4. Krzystolik MG, Afshari MA, Adamis AP, Gaudreault J, Gragoudas ES, Michaud NA, Li W, Connolly E, O'Neill CA, Miller JW. Prevention of experimental choroidal neovascularization with intravitreal anti-vascular endothelial growth factor antibody fragment. *Arch Ophthalmol*. 2002; 120:338–46.
<https://doi.org/10.1001/archophth.120.3.338>
PMID:[11879138](https://pubmed.ncbi.nlm.nih.gov/11879138/)
5. Kwak N, Okamoto N, Wood JM, Campochiaro PA. VEGF is major stimulator in model of choroidal neovascularization. *Invest Ophthalmol Vis Sci*. 2000; 41:3158–64.
PMID:[10967078](https://pubmed.ncbi.nlm.nih.gov/10967078/)
6. Schlingemann RO. Role of growth factors and the wound healing response in age-related macular degeneration. *Graefes Arch Clin Exp Ophthalmol*. 2004; 242:91–101.
<https://doi.org/10.1007/s00417-003-0828-0>
PMID:[14685874](https://pubmed.ncbi.nlm.nih.gov/14685874/)
7. Beatty S, Koh H, Phil M, Henson D, Boulton M. The role of oxidative stress in the pathogenesis of age-related macular degeneration. *Surv Ophthalmol*. 2000; 45:115–34.
[https://doi.org/10.1016/s0039-6257\(00\)00140-5](https://doi.org/10.1016/s0039-6257(00)00140-5)
PMID:[11033038](https://pubmed.ncbi.nlm.nih.gov/11033038/)
8. Grossniklaus HE, Ling JX, Wallace TM, Dithmar S, Lawson DH, Cohen C, Elnor VM, Elnor SG, Sternberg P Jr. Macrophage and retinal pigment epithelium expression of angiogenic cytokines in choroidal neovascularization. *Mol Vis*. 2002; 8:119–26.
PMID:[11979237](https://pubmed.ncbi.nlm.nih.gov/11979237/)
9. Roh MI, Kim HS, Song JH, Lim JB, Koh HJ, Kwon OW. Concentration of cytokines in the aqueous humor of patients with naive, recurrent and regressed CNV associated with amd after bevacizumab treatment. *Retina*. 2009; 29:523–9.
<https://doi.org/10.1097/IAE.0b013e318195cb15>
PMID:[19262441](https://pubmed.ncbi.nlm.nih.gov/19262441/)
10. Campa C, Costagliola C, Incorvaia C, Sheridan C, Semeraro F, De Nadai K, Sebastiani A, Parmeggiani F. Inflammatory mediators and angiogenic factors in choroidal neovascularization: pathogenetic interactions and therapeutic implications. *Mediators Inflamm*. 2010; 2010:546826.
<https://doi.org/10.1155/2010/546826>
PMID:[20871825](https://pubmed.ncbi.nlm.nih.gov/20871825/)
11. Mares-Perlman JA, Brady WE, Klein R, VandenLangenberg GM, Klein BE, Palta M. Dietary fat and age-related maculopathy. *Arch Ophthalmol*. 1995; 113:743–8.
<https://doi.org/10.1001/archophth.1995.01100060069034>
PMID:[7786215](https://pubmed.ncbi.nlm.nih.gov/7786215/)
12. Chew EY, Klein ML, Ferris FL 3rd, Remaley NA, Murphy RP, Chantry K, Hoogwerf BJ, Miller D. Association of elevated serum lipid levels with retinal hard exudate in diabetic retinopathy. Early Treatment Diabetic Retinopathy Study (ETDRS) Report 22. *Arch Ophthalmol*. 1996; 114:1079–84.
<https://doi.org/10.1001/archophth.1996.01100140281004>
PMID:[8790092](https://pubmed.ncbi.nlm.nih.gov/8790092/)
13. McKay GJ, Patterson CC, Chakravarthy U, Dasari S, Klaver CC, Vingerling JR, Ho L, de Jong PT, Fletcher AE, Young IS, Seland JH, Rahu M, Soubrane G, et al. Evidence of association of APOE with age-related macular degeneration: a pooled analysis of 15 studies. *Hum Mutat*. 2011; 32:1407–16.
<https://doi.org/10.1002/humu.21577>
PMID:[21882290](https://pubmed.ncbi.nlm.nih.gov/21882290/)
14. Wang L, Clark ME, Crossman DK, Kojima K, Messinger JD, Mobley JA, Curcio CA. Abundant lipid and protein components of drusen. *PLoS One*. 2010; 5:e10329.
<https://doi.org/10.1371/journal.pone.0010329>
PMID:[20428236](https://pubmed.ncbi.nlm.nih.gov/20428236/)

15. Malek G, Li CM, Guidry C, Medeiros NE, Curcio CA. Apolipoprotein B in cholesterol-containing drusen and basal deposits of human eyes with age-related maculopathy. *Am J Pathol.* 2003; 162:413–25.
[https://doi.org/10.1016/S0002-9440\(10\)63836-9](https://doi.org/10.1016/S0002-9440(10)63836-9)
PMID:12547700
16. Curcio CA, Johnson M, Huang JD, Rudolf M. Aging, age-related macular degeneration, and the response-to-retention of apolipoprotein B-containing lipoproteins. *Prog Retin Eye Res.* 2009; 28:393–422.
<https://doi.org/10.1016/j.preteyeres.2009.08.001>
PMID:19698799
17. Bitsch F, Aichholz R, Kallen J, Geisse S, Fournier B, Schlaeppi JM. Identification of natural ligands of retinoic acid receptor-related orphan receptor alpha ligand-binding domain expressed in Sf9 cells—a mass spectrometry approach. *Anal Biochem.* 2003; 323:139–49.
<https://doi.org/10.1016/j.ab.2003.08.029>
PMID:14622968
18. Kallen J, Schlaeppi JM, Bitsch F, Delhon I, Fournier B. Crystal structure of the human RORalpha Ligand binding domain in complex with cholesterol sulfate at 2.2 Å. *J Biol Chem.* 2004; 279:14033–8.
<https://doi.org/10.1074/jbc.M400302200>
PMID:14722075
19. Jun G, Nicolaou M, Morrison MA, Buros J, Morgan DJ, Radeke MJ, Yonekawa Y, Tsironi EE, Kotoula MG, Zacharaki F, Mollema N, Yuan Y, Miller JW, et al. Influence of ROBO1 and RORA on risk of age-related macular degeneration reveals genetically distinct phenotypes in disease pathophysiology. *PLoS One.* 2011; 6:e25775.
<https://doi.org/10.1371/journal.pone.0025775>
PMID:21998696
20. Silveira AC, Morrison MA, Ji F, Xu H, Reinecke JB, Adams SM, Arneberg TM, Janssian M, Lee JE, Yuan Y, Schaumberg DA, Kotoula MG, Tsironi EE, et al. Convergence of linkage, gene expression and association data demonstrates the influence of the RAR-related orphan receptor alpha (RORA) gene on neovascular AMD: a systems biology based approach. *Vision Res.* 2010; 50:698–715.
<https://doi.org/10.1016/j.visres.2009.09.016>
PMID:19786043
21. Schaumberg DA, Chasman D, Morrison MA, Adams SM, Guo Q, Hunter DJ, Hankinson SE, DeAngelis MM. Prospective study of common variants in the retinoic acid receptor-related orphan receptor α gene and risk of neovascular age-related macular degeneration. *Arch Ophthalmol.* 2010; 128:1462–71.
<https://doi.org/10.1001/archophthalmol.2010.261>
PMID:21060049
22. Jetten AM. Retinoid-related orphan receptors (RORs): critical roles in development, immunity, circadian rhythm, and cellular metabolism. *Nucl Recept Signal.* 2009; 7:e003.
<https://doi.org/10.1621/nrs.07003>
PMID:19381306
23. Jetten AM, Kurebayashi S, Ueda E. The ROR nuclear orphan receptor subfamily: critical regulators of multiple biological processes. *Prog Nucleic Acid Res Mol Biol.* 2001; 69:205–47.
[https://doi.org/10.1016/s0079-6603\(01\)69048-2](https://doi.org/10.1016/s0079-6603(01)69048-2)
PMID:11550795
24. Vu-Dac N, Gervois P, Grötzinger T, De Vos P, Schoonjans K, Fruchart JC, Auwerx J, Mariani J, Tedgui A, Staels B. Transcriptional regulation of apolipoprotein A-I gene expression by the nuclear receptor RORalpha. *J Biol Chem.* 1997; 272:22401–4.
<https://doi.org/10.1074/jbc.272.36.22401>
PMID:9278389
25. Raspé E, Duez H, Gervois P, Fiévet C, Fruchart JC, Besnard S, Mariani J, Tedgui A, Staels B. Transcriptional regulation of apolipoprotein C-III gene expression by the orphan nuclear receptor RORalpha. *J Biol Chem.* 2001; 276:2865–71.
<https://doi.org/10.1074/jbc.M004982200>
PMID:11053433
26. Crumbley C, Wang Y, Banerjee S, Burris TP. Regulation of expression of citrate synthase by the retinoic acid receptor-related orphan receptor α (ROR α). *PLoS One.* 2012; 7:e33804.
<https://doi.org/10.1371/journal.pone.0033804>
PMID:22485150
27. Solt LA, Kumar N, Nuhant P, Wang Y, Lauer JL, Liu J, Istrate MA, Kamenecka TM, Roush WR, Vidović D, Schürer SC, Xu J, Wagoner G, et al. Suppression of TH17 differentiation and autoimmunity by a synthetic ROR ligand. *Nature.* 2011; 472:491–4.
<https://doi.org/10.1038/nature10075>
PMID:21499262
28. Journiac N, Jolly S, Jarvis C, Gautheron V, Rogard M, Trembleau A, Blondeau JP, Mariani J, Vernet-der Garabedian B. The nuclear receptor ROR(alpha) exerts a bi-directional regulation of IL-6 in resting and reactive astrocytes. *Proc Natl Acad Sci U S A.* 2009; 106:21365–70.
<https://doi.org/10.1073/pnas.0911782106>
PMID:19955433
29. Delerive P, Monté D, Dubois G, Trottein F, Fruchart-Najib J, Mariani J, Fruchart JC, Staels B. The orphan nuclear receptor ROR alpha is a negative regulator of the inflammatory response. *EMBO Rep.* 2001; 2:42–8.
<https://doi.org/10.1093/embo-reports/kve007>
PMID:11252722

30. Wang R, Campbell S, Amir M, Mosure SA, Bassette MA, Eliason A, Sundrud MS, Kamenecka TM, Solt LA. Genetic and pharmacological inhibition of the nuclear receptor ROR α regulates T_H17 driven inflammatory disorders. *Nat Commun.* 2021; 12:76.
<https://doi.org/10.1038/s41467-020-20385-9>
PMID:33397953
31. Ino H. Immunohistochemical characterization of the orphan nuclear receptor ROR alpha in the mouse nervous system. *J Histochem Cytochem.* 2004; 52:311–23.
<https://doi.org/10.1177/002215540405200302>
PMID:14966198
32. Tosini G, Davidson AJ, Fukuhara C, Kasamatsu M, Castanon-Cervantes O. Localization of a circadian clock in mammalian photoreceptors. *FASEB J.* 2007; 21:3866–71.
<https://doi.org/10.1096/fj.07-8371com>
PMID:17621597
33. Steinmayr M, André E, Conquet F, Rondi-Reig L, Delhaye-Bouchaud N, Auclair N, Daniel H, Crépel F, Mariani J, Sotelo C, Becker-André M. staggerer phenotype in retinoid-related orphan receptor alpha-deficient mice. *Proc Natl Acad Sci U S A.* 1998; 95:3960–5.
<https://doi.org/10.1073/pnas.95.7.3960>
PMID:9520475
34. Sun Y, Liu CH, SanGiovanni JP, Evans LP, Tian KT, Zhang B, Stahl A, Pu WT, Kamenecka TM, Solt LA, Chen J. Nuclear receptor ROR α regulates pathologic retinal angiogenesis by modulating SOCS3-dependent inflammation. *Proc Natl Acad Sci U S A.* 2015; 112:10401–6.
<https://doi.org/10.1073/pnas.1504387112>
PMID:26243880
35. Sun Y, Liu CH, Wang Z, Meng SS, Burnim SB, SanGiovanni JP, Kamenecka TM, Solt LA, Chen J. ROR α modulates semaphorin 3E transcription and neurovascular interaction in pathological retinal angiogenesis. *FASEB J.* 2017; 31:4492–502.
<https://doi.org/10.1096/fj.201700172R>
PMID:28646017
36. Hamilton BA, Frankel WN, Kerrebrock AW, Hawkins TL, FitzHugh W, Kusumi K, Russell LB, Mueller KL, van Berkel V, Birren BW, Kruglyak L, Lander ES. Disruption of the nuclear hormone receptor RORalpha in staggerer mice. *Nature.* 1996; 379:736–9.
<https://doi.org/10.1038/379736a0>
PMID:8602221
37. Gong Y, Li J, Sun Y, Fu Z, Liu CH, Evans L, Tian K, Saba N, Fredrick T, Morss P, Chen J, Smith LE. Optimization of an Image-Guided Laser-Induced Choroidal Neovascularization Model in Mice. *PLoS One.* 2015; 10:e0132643.
<https://doi.org/10.1371/journal.pone.0132643>
PMID:26161975
38. Liu CH, Sun Y, Li J, Gong Y, Tian KT, Evans LP, Morss PC, Fredrick TW, Saba NJ, Chen J. Endothelial microRNA-150 is an intrinsic suppressor of pathologic ocular neovascularization. *Proc Natl Acad Sci U S A.* 2015; 112:12163–8.
<https://doi.org/10.1073/pnas.1508426112>
PMID:26374840
39. Espinosa-Heidmann DG, Marin-Castano ME, Pereira-Simon S, Hernandez EP, Elliot S, Cousins SW. Gender and estrogen supplementation increases severity of experimental choroidal neovascularization. *Exp Eye Res.* 2005; 80:413–23.
<https://doi.org/10.1016/j.exer.2004.10.008>
PMID:15721623
40. Li J, Liu CH, Sun Y, Gong Y, Fu Z, Evans LP, Tian KT, Juan AM, Hurst CG, Mammoto A, Chen J. Endothelial TWIST1 promotes pathological ocular angiogenesis. *Invest Ophthalmol Vis Sci.* 2014; 55:8267–77.
<https://doi.org/10.1167/iovs.14-15623>
PMID:25414194
41. Kumar N, Kojetin DJ, Solt LA, Kumar KG, Nuhant P, Duckett DR, Cameron MD, Butler AA, Roush WR, Griffin PR, Burris TP. Identification of SR3335 (ML-176): a synthetic ROR α selective inverse agonist. *ACS Chem Biol.* 2011; 6:218–22.
<https://doi.org/10.1021/cb1002762>
PMID:21090593
42. Wang Y, Kumar N, Nuhant P, Cameron MD, Istrate MA, Roush WR, Griffin PR, Burris TP. Identification of SR1078, a synthetic agonist for the orphan nuclear receptors ROR α and ROR γ . *ACS Chem Biol.* 2010; 5:1029–34.
<https://doi.org/10.1021/cb100223d>
PMID:20735016
43. Doebelin C, He Y, Campbell S, Nuhant P, Kumar N, Koenig M, Garcia-Ordóñez R, Chang MR, Roush WR, Lin L, Kahn S, Cameron MD, Griffin PR, et al. Discovery and Optimization of a Series of Sulfonamide Inverse Agonists for the Retinoic Acid Receptor-Related Orphan Receptor- α . *Med Chem.* 2019; 15:676–84.
<https://doi.org/10.2174/1573406415666190222124745>
PMID:30799793
44. Shao Z, Friedlander M, Hurst CG, Cui Z, Pei DT, Evans LP, Juan AM, Tahiri H, Duhamel F, Chen J, Sapienza P, Chemtob S, Joyal JS, Smith LE. Choroid sprouting assay: an ex vivo model of microvascular angiogenesis. *PLoS One.* 2013; 8:e69552.
<https://doi.org/10.1371/journal.pone.0069552>
PMID:23922736

45. Wang Z, Yemanyi F, Blomfield AK, Bora K, Huang S, Liu CH, Britton WR, Cho SS, Tomita Y, Fu Z, Ma JX, Li WH, Chen J. Amino acid transporter SLC38A5 regulates developmental and pathological retinal angiogenesis. *Elife*. 2022; 11:e73105.
<https://doi.org/10.7554/eLife.73105>
PMID:36454214
46. Liu CH, Wang Z, Huang S, Sun Y, Chen J. MicroRNA-145 Regulates Pathological Retinal Angiogenesis by Suppression of TMOD3. *Mol Ther Nucleic Acids*. 2019; 16:335–47.
<https://doi.org/10.1016/j.omtn.2019.03.001>
PMID:30981984
47. Huang S, Liu CH, Wang Z, Fu Z, Britton WR, Blomfield AK, Kamenecka TM, Dunaief JL, Solt LA, Chen J. REV-ERB α regulates age-related and oxidative stress-induced degeneration in retinal pigment epithelium via NRF2. *Redox Biol*. 2022; 51:102261.
<https://doi.org/10.1016/j.redox.2022.102261>
PMID:35176707
48. Wang Z, Liu CH, Huang S, Fu Z, Tomita Y, Britton WR, Cho SS, Chen CT, Sun Y, Ma JX, He X, Chen J. Wnt signaling activates MFSD2A to suppress vascular endothelial transcytosis and maintain blood-retinal barrier. *Sci Adv*. 2020; 6:eaba7457.
<https://doi.org/10.1126/sciadv.aba7457>
PMID:32923627
49. Sainson RC, Johnston DA, Chu HC, Holderfield MT, Nakatsu MN, Crampton SP, Davis J, Conn E, Hughes CC. TNF primes endothelial cells for angiogenic sprouting by inducing a tip cell phenotype. *Blood*. 2008; 111:4997–5007.
<https://doi.org/10.1182/blood-2007-08-108597>
PMID:18337563
50. Besnard S, Heymes C, Merval R, Rodriguez M, Galizzi JP, Boutin JA, Mariani J, Tedgui A. Expression and regulation of the nuclear receptor ROR α in human vascular cells. *FEBS Lett*. 2002; 511:36–40.
[https://doi.org/10.1016/s0014-5793\(01\)03275-6](https://doi.org/10.1016/s0014-5793(01)03275-6)
PMID:11821045
51. Besnard S, Silvestre JS, Duriez M, Bakouche J, Lemaigre-Dubreuil Y, Mariani J, Levy BI, Tedgui A. Increased ischemia-induced angiogenesis in the staggerer mouse, a mutant of the nuclear receptor ROR α . *Circ Res*. 2001; 89:1209–15.
<https://doi.org/10.1161/hh2401.101755>
PMID:11739287
52. Lichtlen P, Lam TT, Nork TM, Streit T, Urech DM. Relative contribution of VEGF and TNF- α in the cynomolgus laser-induced CNV model: comparing the efficacy of bevacizumab, adalimumab, and ESBA105. *Invest Ophthalmol Vis Sci*. 2010; 51:4738–45.
<https://doi.org/10.1167/iov.09-4890>
PMID:20393113
53. Surjit M, Ganti KP, Mukherji A, Ye T, Hua G, Metzger D, Li M, Chambon P. Widespread negative response elements mediate direct repression by agonist-liganded glucocorticoid receptor. *Cell*. 2011; 145:224–41.
<https://doi.org/10.1016/j.cell.2011.03.027>
PMID:21496643
54. Peavey J, Parmar VM, Malek G. Correction: Peavey et al. Nuclear Receptor Atlases of Choroidal Tissues Reveal Candidate Receptors Associated with Age-Related Macular Degeneration. *Cells* 2022, 11, 2386. *Cells*. 2022; 11:3948.
<https://doi.org/10.3390/cells11243948>
PMID:36552901
55. Apte RS, Richter J, Herndon J, Ferguson TA. Macrophages inhibit neovascularization in a murine model of age-related macular degeneration. *PLoS Med*. 2006; 3:e310.
<https://doi.org/10.1371/journal.pmed.0030310>
PMID:16903779
56. Fujieda H, Bremner R, Mears AJ, Sasaki H. Retinoic acid receptor-related orphan receptor alpha regulates a subset of cone genes during mouse retinal development. *J Neurochem*. 2009; 108:91–101.
<https://doi.org/10.1111/j.1471-4159.2008.05739.x>
PMID:19014374
57. Solt LA, Burris TP. Action of RORs and their ligands in (patho)physiology. *Trends Endocrinol Metab*. 2012; 23:619–27.
<https://doi.org/10.1016/j.tem.2012.05.012>
PMID:22789990
58. Rodriguez IR, Clark ME, Lee JW, Curcio CA. 7-ketocholesterol accumulates in ocular tissues as a consequence of aging and is present in high levels in drusen. *Exp Eye Res*. 2014; 128:151–5.
<https://doi.org/10.1016/j.exer.2014.09.009>
PMID:25261634